DOI 10.7343/as-2022-568

ACQUE SOTTERRANEE
Italian Journal of Groundwater
journal homepage: https://www.acquesotterranee.net/

2022-AS42-568: 41- 51

Investigating the feasibility of using precipitation measurements from weather RaDAR to estimate potential recharge in regional aquifers: the Majella massif case study in Central Italy

Indagare la fattibilità dell'utilizzo di misure di precipitazioni da RaDAR meteorologico per stimare la ricarica potenziale nelle falde acquifere regionali: il caso studio del massiccio della Majella nel centro Italia

Diego Di Curzio[a], Alessia Di Giovanni[a], Raffaele Lidori[b], Frank Silvio Marzano[b,c], Sergio Rusi[a,b]

[a] Department of Engineering and Geology, University "G. d'Annunzio", Chieti-Pescara- email: *alessia.digiovanni@unich.it; diego.dicurzio@unich.it*
[b] Center of Excellence Telesensing of Environment and Model Prediction of Severe events - email: *raffaele.lidori@gmail.com; sergio.rusi@unich.it.*
[c] Department of Information Engineering, Sapienza University of Rome

ARTICLE INFO

Ricevuto/*Received*: 28 April 2022
Accettato/*Accepted*: 26 September 2022
Pubblicato online/*Published online*: 30 September 2022

Handling Editor:
Manuela Lasagna

Publication note:
This contribution has been selected from Flowpath 2021 congress held in Naples 1-3 December 2021

Citation:
Di Curzio D, Di Giovanni A, Lidori R, Marzano FS, Rusi S (2022) Investigating the feasibility of using precipitation measurements from weather radar to estimate recharge in regional aquifers: the Majella massif case study in Central Italy. Acque Sotterranee - *Italian Journal of Groundwater*, 11(3), 41 - 51
https://doi.org/10.7343/as-2022-568

Correspondence to:
Alessia Di Giovanni
alessia.digiovanni@unich.it

Keywords: *rainfall, weather RaDAR, aquifer potential recharge, water budget, Majella massif.*

Parole chiave: precipitazioni, RaDAR metereologico, ricarica potenziale degli acquiferi, bilancio idrico, Majella.

Riassunto

La mancanza di continuità spaziale e temporale nella rete dei pluviometri rappresenta l'ostacolo principale per stime di ricarica affidabili. Negli anni passati, l'uso del RaDAR meteorologico basato sulle microonde ha enormemente migliorato la stima quantitativa delle precipitazioni, fornendo stime spazialmente continue delle precipitazioni su un'area di oltre 400 km^2 ogni 10 minuti; inoltre, il RaDAR meteorologico ha dato prova di affidabilità anche in aree montuose.

Queste caratteristiche dei dati di precipitazione, derivanti dal RaDAR, potrebbero migliorare la stima della ricarica potenziale delle falde acquifere che generalmente si basano su geospazializzazioni dei dati di pioggia (ad es. i poligoni di Thiessen) misurati da stazioni sparse sul territorio e che molto spesso non presenta stazioni di misura a quote elevate, ossia nelle aree di ricarica, e così da aumentare il grado di incertezza nella valutazione dei volumi in ingresso; come già discusso in letteratura, anche le stime ottenute dal RaDAR meteorologico presentano delle possibilità di errore che, tuttavia, possono essere ridotte attraverso opportune elaborazioni, pur mantenendo alcune incertezze sulla stima del tasso di pioggia in superficie.

Lo scopo di questo lavoro, nonostante gli attualmente necessari complessi procedimenti numerici, è quello di valutare l'utilizzo di dati misurati dal RaDAR meteorologico come alternativa o integrazione all'uso di quelli pluviometrici. Sulla base delle considerazioni precedenti, è stato valutato l'utilizzo di dati RaDAR per stimare la ricarica potenziale delle falde acquifere e calcolare un bilancio idrico dettagliato nelle aree caratterizzate da altitudini elevate, come il massiccio della Majella nell'Appennino centrale.

Il bilancio idrologico è stato calcolato negli anni 2017 e 2018, utilizzando sia i dati di precipitazione da RaDAR meteorologico che da pluviometro, attraverso i metodi di Turc e Thornthwaite. Nonostante le incertezze citate, i dati RaDAR restituiscono risultati affidabili e coerenti come evidenza il confronto con il bilancio idrico, ottenuto sia dai dati del pluviometro che dai dati sperimentali già noti in letteratura. Questo lavoro interdisciplinare può spianare la strada per il monitoraggio continuo della ricarica potenziale delle falde acquifere ad un'altissima risoluzione temporale e spaziale.

Abstract

Rain gauge spatial sparsity and temporal discontinuity of data represent one of the major issues for reliable recharge estimations. In the past decades, the use of ground-based microwave weather RaDAR has dramatically improved quantitative rainfall estimation by providing spatially continuous estimates of rainfall over an area of more than 400 km^2 every 10 minutes. Furthermore, weather RaDAR data have also proved relatively reliable in mountainous areas. These paramount features of RaDAR-derived precipitation data could improve the estimation of potential recharge of aquifers, which rely on geospatializations (e.g., Thiessen polygons) of rainfall data collected by a sparse rain gauge network which often shows lacking at high altitude (i.e., recharge areas), introducing additional uncertainty in the inflow volumes. Weather RaDAR rainfall estimation is also affected by various sources of error, which can be reduced by proper post-processing; however, uncertainties remain, especially for surface rain rate estimations.

Despite the currently necessary complex numerical processing, the purpose of the study is to evaluate the use of the weather RaDAR data as an alternative or in addition to meteorological data. Based on the above considerations, the feasibility of using RaDAR-based precipitation data to estimate aquifer potential recharge and calculate a detailed water budget in the areas characterized by high elevations, such as the Majella massif in the central Apennines, has been evaluated.

To address this objective, the water budget has been calculated in the 2017-2018 period using both RaDAR-based precipitation data and rain gauge data, as well as adopting different methods (i.e., Turc and Thornthwaite). Although intrinsically uncertain, the RaDAR-based precipitation data provided solid results, pointed out by comparing it with water budget obtained by rain gauge data, and especially with experimental literature data. This interdisciplinary work may pave the way for continuous monitoring of aquifer potential recharge at extremely high temporal and spatial resolution.

Introduction

Rainfall data, recorded by traditional rain gauge networks, show many limitations due to an inhomogeneous discrete distribution of the measuring stations, leading to temporal and spatial gaps inside the available datasets (Navarro et al. 2020). Indeed, in the Central Apennines (Abruzzo region, Central Italy), rain gauge stations are mostly distributed in river plains and foothill areas (sometimes used for hydrogeological purpose like in Chiaudani et al. 2017 and Di Curzio et al. 2021) but rarely at altitudes higher than 1500 m above the sea level (a.s.l.), which often represent the recharge areas of the most important regional aquifers (Andreo et al. 2008; Petitta et al. 2010; Fronzi et al. 2020; Lorenzi et al. 2022). This implies that the estimation of the aquifers' potential recharge for these elevated zones must be calculated with indirect methods.

Spatial distribution of rainfall from rain gauge network data can be reconstructed using spatialization techniques, such as the simple Thiessen polygons (Thiessen 1911), or by way of more sophisticated geostatistical methods (i.e., kriging or stochastic simulation methods), which also provide a quantification of the estimation uncertainty (Wackernagel 2003; Chilès and Delfiner 2012; Di Curzio et al. 2019; Vessia et al. 2020). In any case, the interpolation accuracy of spatialized rainfall data strongly depends on the spatial density and spacing of the rain gauge network itself (McKee and Binns 2016). Furthermore, rain dataset temporal continuity must be evaluated as well since in long time series missing data are likely to occur. This implies that precipitation records are not always continuous over time, and sometimes months or even years of them are missing resulting in a loss of reliability, especially in the aquifer potential recharge estimation and water budget assessment (Viaroli et al. 2018; Viaroli et al. 2019).

A viable alternative for rainfall measurement are the microwave weather RaDAR (Radio Detection And Ranging) remote sensing systems (Falconi and Marzano 2019), which provide high spatial and temporal frequency dataset of rainfall intensity: RaDAR recordings are typically every 10 minutes and spatial resolution is from 125 m up to 500 m (Barbieri et al. 2022). Weather RaDAR allows a real-time estimation of rainfall intensity up to 200 km from the instrument location, identifying the hydrometeors type (i.e., rain, snow, hail) as well as estimating rain cloud velocity and direction.

These systems are generally used for extreme weather surveillance, assimilation into hydrological and meteorological numerical models, and monitoring the volcanic eruption clouds as well as for supporting Civil Protection agencies (e.g., Vulpiani et al. 2012; Montopoli et al. 2021). However, literature regarding applications for hydrogeological purposes is nihil.

Weather RaDAR measurement can be affected by errors as well: ground targets can cause echoes, called "ground clutter", which may be misinterpreted as rainfall such as buildings, hills, and mountains (Falconi and Marzano 2019). These artifacts can be detected by using RaDAR mapping features and mitigated and/or corrected through ad hoc signal processing (Barbieri et al. 2022). On the other hand, RaDAR-derived rainfall datasets can provide the reduction of uncertainty about inflow volumes due to its spatial-temporal resolution, which is definitely much higher than rain gauge networks. In this respect, exploiting the aquifer annual potential recharge estimation is expected to be more accurate, especially at high altitudes.

According to what has just been discussed, this research aims at testing the reliability and feasibility of the use of novel weather RaDAR data to quantify the groundwater recharge and budget, by comparing them with the ones collected by rain gauges. As a test area, the well-known Majella massif (Nanni and Rusi 2003; Fiorillo et al. 2015; Chiaudani et al. 2019) has been selected. Since the objective of this research is to assess quality of data, the Thiessen method has been selected as common data support to compare two different types of rainfall dataset that would have not been possible to compare otherwise (i.e., point and raster data), even though it is the simplest of the existing spatialization techniques.

In consideration of the possibility of using more advanced geostatistical interpolation techniques, in the present work it has nevertheless been used in order to compare the results obtained with those known in the scientific literature from similar elaborations.

Material and methods

Study area

The Majella massif is located in the Central Apennines (Italy), and its altitude reaches almost 3000 m a.s.l. (Fig. 1). From a geological point of view, the Majella is an asymmetric anticline sited in the outer part of central Apennines and made up by a thick Jurassic – Miocene carbonate sequence (about 2 km), under an Upper Miocene–Middle Pliocene silicoclastic deposits (Nanni and Rusi 2003; Tondi et al. 2006; Fiorillo et al. 2015; Chiaudani et al. 2019).

From a hydrogeological point of view, the Majella carbonatic massif is one of the most important groundwater bodies in Central Apennines and one of the largest with an extension of 273 km^2 in outcrop (Chiaudani et al. 2019). In these kinds of aquifers primary conductivity is lower than secondary; indeed, the last one is related to the orogenic processes that affect the Apennines through Neogene and Plio - Quaternary periods causing intense deformation and fracturing inside carbonatic deposits.

Five hydrogeological complexes have been identified (Nanni and Rusi 2003):

- a hydrogeological complex of Jurassic-Paleocene limestone characterized by high permeability due to karst and fissuring;
- an aquiclude of marly limestone and marlstone of the Bolognano Formation;
- a hydrogeological complex of calcarenite of the Bolognano Formation characterized by variable permeability, decreasing northward, caused by fracturing and porosity;
- an aquiclude of terrigenous and evaporitic formations consisting of clay, marl and marly clay;

- a hydrogeological complex of highly permeable continental detritus.

This hydrogeological complex arrangement leads to a regional aquifer in which several secondary perched aquifers can be found. The basal aquifer recharge is entirely due to rainfall and snowmelt infiltration, which is fostered by the presence of wide karst plains on the top and detrital deposits. Over 240 springs can be found across the entire Majella massif; however, the basal springs are on the eastern and northern sides, with average discharges ranging from 0.6 to 2.6 m^3/s and the mean total discharge equal to about 8 m^3/s. Furthermore, data from literature (Nanni and Rusi 2003; Boni et al. 1986) indicate that the infiltration rate is about 922 mm/year related to a rainfall rate of about 1520 mm/year, suggesting the absence of underground groundwater recharge from the neighboring regional aquifers.

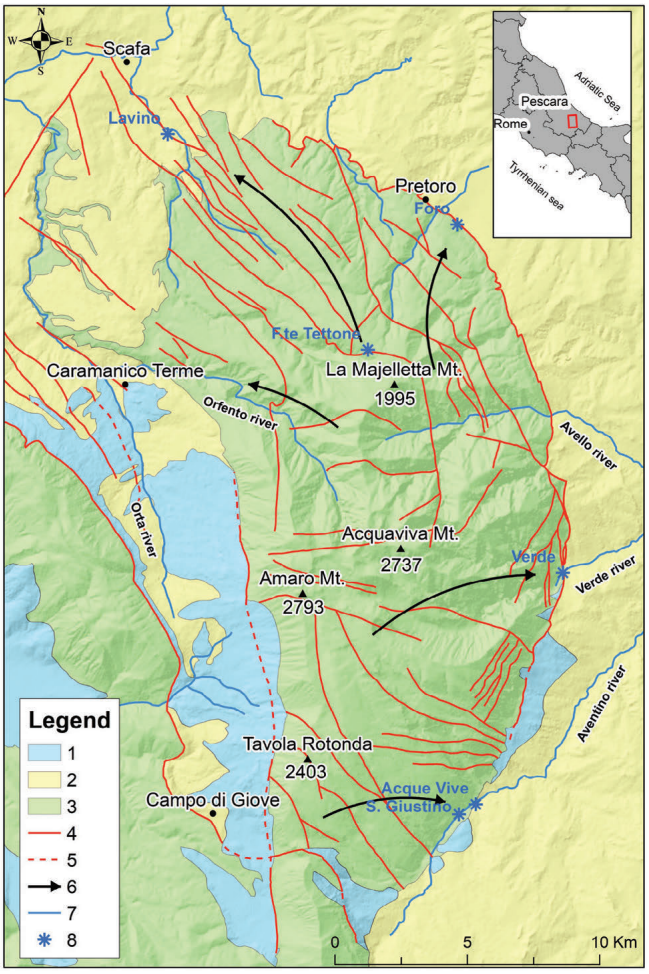

Fig. 1 - Majella massif study area and schematic hydrogeological framework. 1. Carbonatic complex (high permeable Bolognano formation), aquifer; 2. continental detritus complex, aquifer; 3. clayey deposits, aquiclude; 4. faults; 5. buried faults; 6. main flow paths; 7. main streams; 8. main basal springs.

Fig. 1 - Area di studio del massiccio della Majella e assetto idrogeologico schematico. 1. Complesso carbonatico (formazione di Bolognano molto permeabile), acquifero; 2. complesso dei depositi continentali, acquifero; 3. complesso dei depositi argillosi, aquiclude; 4. faglie certe; 5. faglie sepolte; 6. direzioni di flussi principali; 7. corsi d'acqua principali; 8. sorgenti basali principali.

Evaluation of rainfall from gauging stations

Rainfall data from nine automatic gauging stations all over Majella massif (Fig. 2) have been considered in a time window of two-years (2017 - 2018); these datasets have been provided by the Hydrographic Service of Abruzzo Region, which owns the regional rain gauge network installed just after the World War II. The stations' location has not changed over the time (Chiaudani et al. 2019). Moreover, they are sited at elevation below 1500 m a.s.l., hence, following the procedures for using the Thiessen method, three virtual stations have been introduced to fill the lack in Majella area: Monte Amaro (MAR*), Monte Focalone (MFO*) and Tavola Rotonda (TRO*).

The twelve gauging stations' positions have been used to draw the Thiessen polygons around the study area; rainfall raw data from the nine gauging stations inside and adjacent the Majella hydrostructure (PAL, GUR, PTR, CSD, SLM, ASI, SLE, CRM, PLN) were cumulated to monthly and annual resolution; datasets for the three virtual stations (TRO*, MFO*, MAR*) were obtained from regression lines built from real rainfall records for every considered month and year. Anyway, only six real stations (PAL, GUR, PTR, CSD, CRM, PLN) and the three virtual ones have been used for estimations, because their Thiessen polygons are inside Majella hydrostructure border. Temperature data were processed such as rainfall ones.

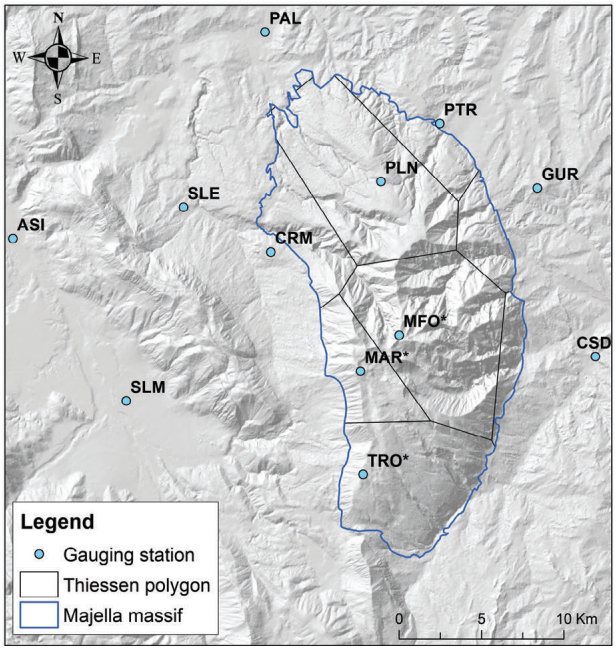

Fig. 2 - Majella massif study area and rain gauging stations used for Thiessen polygons. PAL, Pescara ad Alanno; PRT, Pretoro; GUR, Guardiagrele; CSD, Casoli Diga; SLM, Sulmona; ASI, Aterno Sagittario ad Alloggiamento Idroelettrico; SLE, Salle; CRM, Caramanico; PLN, Passo Lanciano; MFO, Monte Focalone; MAR*, Monte Amaro; TRO*, Tavola Rotonda. The asterisk indicates virtual stations.*

Fig. 2 - Area di studio del massiccio della Majella e le stazioni pluviometriche utilizzate per realizzare i topoieti. PAL, Pescara ad Alanno; PRT, Pretoro; GUR, Guardiagrele; CSD, Casoli Diga; SLM, Sulmona; ASI, Aterno Sagittario ad Alloggiamento Idroelettrico; SLE, Salle; CRM, Caramanico; PLN, Passo Lanciano; MFO*, Monte Focalone; MAR*, Monte Amaro; TRO*, Tavola Rotonda. L'asterisco indica le stazioni fittizie.

Evaluation of rainfall from weather RaDAR

Weather RaDAR runs releasing electromagnetic waves into the atmosphere to detect hydrometeors like rain, snow, or hail; the interaction between emitted microwaves and the hydrometeors causes the radiation backscattering, called echo. This signal is converted, after a proper calibration, into the related Surface Rainfall Intensity (SRI), expressed in mm/h, estimated from the RaDAR corrected reflectivity (Z_c) using the equation

$$S_R = \left(10^{\frac{Z_c}{10}}\right)^{\frac{1}{b}} \left(\frac{1}{a}\right)^{\frac{1}{b}} \quad (1)$$

where a and b are two dimensional coefficients geographically calibrated (Falconi and Marzano 2019), and Z_c is conventionally expressed in $mm^6\ m^{-3}$ in Eq. (1).

The C-band weather RaDAR data used in this work are from the Abruzzo Region RaDAR network for a 2017-2018 period (Fig. 3, which illustrates for reference only January 2017 data), such as for rain gauge stations. The limitation to only two years of analysis is justified by the huge amount of data to be processed and to the identification of complete monitoring periods of the meteorological stations. Respect to a few thousand of daily data from rain gauge, the weather RaDAR analysis provides for the processing of tens millions of data for month.

These records are cumulated to a monthly temporal resolution and represented as raster monthly RaDAR maps, as shown in Figure 4 (as in Figure 3, only data for some reference months were reported). Additional annual maps have been provided for both years.

RaDAR data represented in the maps are processed with a composite technique that permits better territory coverage and rainfall quantification; some uncertainties can affect these data: orography or strong precipitation can lead to attenuation or even extinction of the backscattered signal (Barbieri et al. 2022). Using a composite RaDAR data these issues can be overcome, while orography echoes, ground clutter, can be easily and successfully removed using clutter maps; these are generated detecting ground clutter locations when no rain is present and then used to remove clutter from weather RaDAR measurements (Harrison et al. 2000). In relation to the Majella massif, weather RaDAR data have been analyzed using two different approaches, in order to be compared to point rain gauge rainfall data: a point data sampling and a zonal one. In the first case, rainfall data have been sampled from the monthly raster dataset at the gauging station locations, while for the latter a minimum, mean, and maximum value of monthly rainfall intensity has been selected within a certain Thiessen polygon, to include possible three-dimensional features of precipitation events. The same sampling has been made within the annual RaDAR maps for both years.

Aquifer recharge estimation

Rainfall data from gauging stations and weather RaDAR have been both employed for potential recharge volume estimation. Turc and Turc modified, where temperature values were corrected for rain data (Turc 1954), and Thornthwaite and Mather (Thornthwaite and Mather 1957) methods have been applied for evapotranspiration assessment; a 0.85 potential infiltration coefficient has been chosen for karst and fractured limestone (Celico 1983). Infiltration volume has been calculated (Mm^3/yr) using the equation

$$R = I_R\left(P - ET_R\right) \quad (2)$$

where R is the aquifer potential recharge, P is the total rainfall, ET_R is real evapotranspiration, and I_R is the

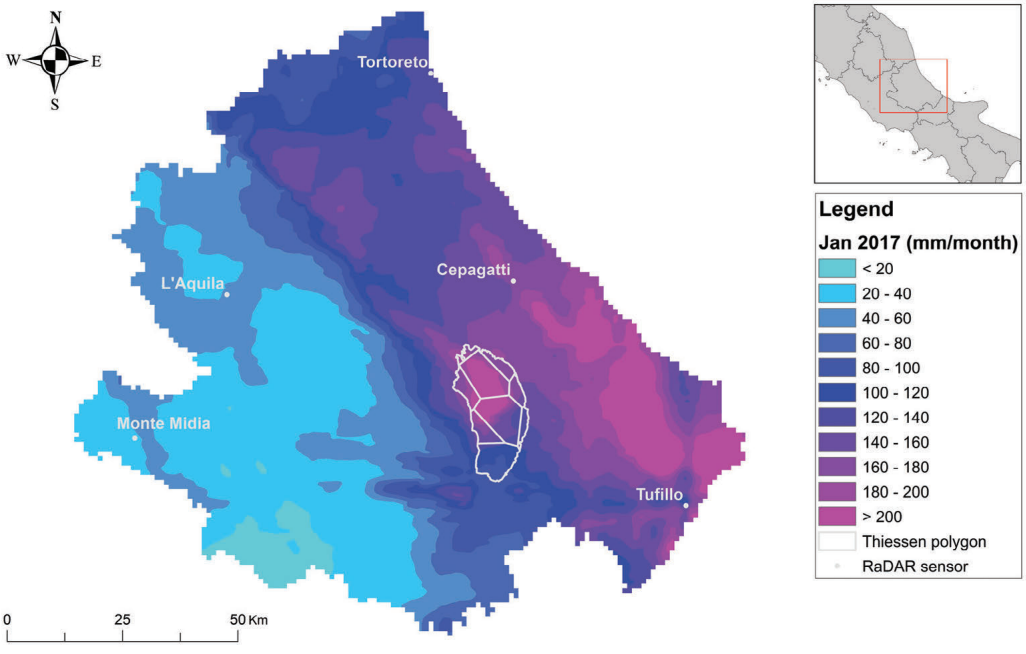

Fig. 3 - Rainfall data from weather RaDAR, January 2017.

Fig. 3 - Rappresentazione dei dati di pioggia da RaDAR meteorologico, gennaio 2017.

infiltration rate. The values obtained were compared with those known in the literature from experimental quantitative surveys although they were obtained in different periods (Nanni and Rusi 2003).

Results

Rainfall evaluation

Monthly and annual rainfall data from the nine gauging stations have been spatialized using the Thiessen polygon method. In Figures 4a, 4c and 4e, 2018 yearly, September 2018 and November 2018 cumulative values of rainfall are displayed, respectively. As can be seen, every polygon area has homogeneous precipitation estimation. On the other hand, Figures 4b, 4d and 4f show 2018 annual rainfall, September 2018 and November 2018 cumulative values from weather RaDAR and inside every Thiessen polygon a range of precipitation values can be found.

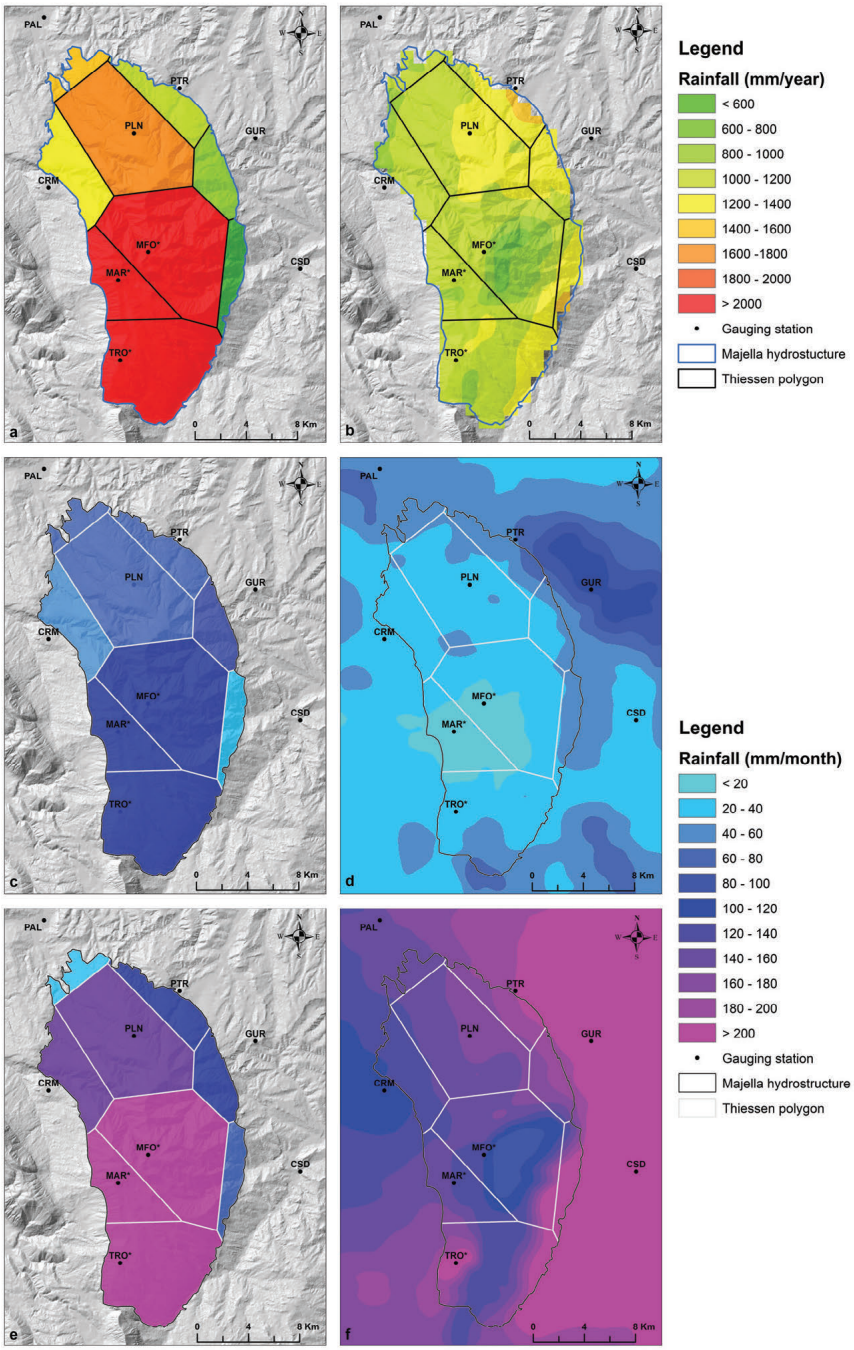

Fig. 4 - Rainfall data output: a. from gauging station, annual cumulate 2018; b. from weather RaDAR, annual cumulate 2018; c. from gauging station, September 2018; d. from weather RaDAR, September 2018; e. from gauging station, November 2018; f. from weather RaDAR, November 2018.

Fig. 4 - Rappresentazione dei dati di pioggia: a. da pluviometro, cumulata annuale 2018; b. da RaDAR, cumulata annuale 2018; c. da pluviometro, settembre 2018; d. da RaDAR, settembre 2018; e. da pluviometro, novembre 2018; f. da RaDAR, novembre 2018.

As above mentioned, these data have been point sampled in rain gauge locations and then maximum, minimum, and mean zonal value calculations have been carried out for each Thiessen polygon. Tables 1a and 1b show the monthly and annual estimation for 2018 from gauging stations and from weather RaDAR.

The greatest discrepancies can be seen at the highest elevations, where the Majella massif recharge area is located. In those sites, the Thiessen polygon spatialization of point rain gauge data shows the highest rainfall rates, whereas the weather RaDAR the lowest ones, pointing out an opposite behavior. Summaries in Table 1a and 1b are consistent with this evidence.

Tab. 1a - Rainfall data from gauging stations and point and zonal sampling from weather RaDAR maps (from January 2018 to July 2018). The asterisk indicates virtual stations.

Tab. 1a - Dati di pioggia misurati da pluviometro e campionati con i due metodi nelle mappe da RaDAR meteorologico (Gennaio 2018 – Luglio 2018). L'asterisco indica le stazioni fittizie.

Data	Station		PAL	GUR	PTR	CSD	CRM	PLN	TRO*	MFC*	MAR*
January	Gauging station		32	--	47	30	53	67	97	105	109
	Point RaDAR		23	39	32	46	30	31	46	45	41
	Zonal RaDAR	Min	22	29	26	39	28	23	37	30	35
		Max	29	33	34	49	39	37	57	45	44
		Mean	24	31	30	44	32	30	44	38	39
February	Gauging station		150	--	214	110	153	206	269	289	297
	Point RaDAR		77	128	106	109	92	82	79	104	101
	Zonal RaDAR	Min	69	66	79	76	76	67	74	63	77
		Max	73	107	111	125	93	94	108	111	110
		Mean	70	84	92	101	89	79	86	84	96
March	Gauging station		53	--	149	45	107	108	177	190	196
	Point RaDAR		88	98	101	100	99	96	181	115	138
	Zonal RaDAR	Min	82	68	75	64	95	76	78	60	99
		Max	86	86	96	88	109	110	361	179	351
		Mean	83	77	85	80	102	94	120	96	149
April	Gauging station		1	--	28	13	34	53	99	110	115
	Point RaDAR		31	28	32	18	29	31	25	30	31
	Zonal RaDAR	Min	27	23	28	19	21	23	23	18	26
		Max	30	39	49	37	35	42	63	47	42
		Mean	29	28	37	25	26	31	41	29	32
May	Gauging station		184	140	198	18	184	304	459	504	523
	Point RaDAR		117	219	207	154	132	195	175	120	124
	Zonal RaDAR	Min	112	213	126	224	119	117	155	96	108
		Max	129	284	240	304	143	244	249	296	209
		Mean	119	233	201	262	129	172	199	172	141
June	Gauging station		138	155	118	34	102	162	240	260	268
	Point RaDAR		68	99	84	96	62	65	34	39	37
	Zonal RaDAR	Min	40	66	46	51	46	42	27	22	27
		Max	58	88	90	90	77	93	76	95	72
		Mean	48	76	64	66	65	61	54	48	38
July	Gauging station		13	20	17	11	13	12	9	10	8
	Point RaDAR		16	61	55	17	19	19	9	24	16
	Zonal RaDAR	Min	18	33	53	19	27	39	24	35	32
		Max	15	24	28	15	16	17	15	18	15
		Mean	15	24	28	15	16	17	15	18	15

Tab. 1b - Rainfall data from gauging stations and point and zonal sampling from weather RaDAR maps (from August 2018 to December 2018 and cumulative values 2018). The asterisk indicates virtual stations.

Tab. 1b - Dati di pioggia misurati da pluviometro e campionati con i due metodi nelle mappe da RaDAR meteorologico (Agosto 2018 – Dicembre 2018 e cumulata 2018). L'asterisco indica le stazioni fittizie.

Data	Station		PAL	GUR	PTR	CSD	CRM	PLN	TRO*	MFC*	MAR*
August	Gauging station		125	35	93	¬¬	128	168	186	197	202
	Point RaDAR		120	62	141	51	134	187	134	129	132
	Zonal RaDAR	Min	70	73	84	86	85	76	113	106	103
		Max	87	207	184	178	208	201	220	216	163
		Mean	77	109	138	117	147	146	165	160	125
September	Gauging station		74	99	76	22	49	67	101	108	111
	Point RaDAR		46	106	57	32	33	39	30	18	17
	Zonal RaDAR	Min	36	34	40	40	30	31	19	9	11
		Max	48	60	68	48	43	46	65	44	30
		Mean	44	40	49	44	35	37	36	26	17
October	Gauging station		248	175	--	122	241	268	145	132	126
	Point RaDAR		173	209	236	166	112	184	105	131	114
	Zonal RaDAR	Min	146	117	179	106	112	127	83	79	93
		Max	199	211	233	161	147	209	136	165	135
		Mean	185	172	207	143	131	168	104	118	118
November	Gauging station		42	110	101	70	143	153	255	277	286
	Point RaDAR		148	225	198	221	113	168	210	120	130
	Zonal RaDAR	Min	140	140	160	139	117	138	127	86	116
		Max	155	197	201	274	142	177	223	249	171
		Mean	150	176	182	208	131	156	165	134	140
December	Gauging station		63	56	43	42	85	97	131	140	144
	Point RaDAR		149	168	201	166	101	206	151	134	140
	Zonal RaDAR	Min	152	69	177	72	112	153	53	28	90
		Max	172	190	203	282	180	206	247	263	179
		Mean	160	165	192	190	144	182	125	120	147
2018	Gauging station		1139	829*	1148*	505*	1334	1707	2259	2420	2489
	Point RaDAR		1055	1443	1449	1175	955	1303	1181	1009	1022
	Zonal RaDAR	Min	972	1154	1049	1108	953	1004	959	722	951
		Max	1037	1322	1518	1446	1157	1338	1390	1383	1255
		Mean	1004	1216	1304	1295	1046	1173	1155	1042	1057

Aquifer potential recharge estimation

Water budget has been calculated for all datasets, for both 2017 and 2018, obtaining recharge volumes. The 2017-year estimation has been carried out with eight stations data instead of nine, because of data lack for GUR station. The results are shown in Table 2 also compared with those known in literature (Nanni and Rusi 2003).

The three methods for water budget estimation show slight discrepancies, in the order of few Mm^3/yr, while differences among the results obtained from the rainfall data sources taken into consideration (i.e., rain gauges data, point and zonal RaDAR data) are significant. This evidence is consistent with what already seen for rainfall data.

Tab. 2 - Infiltration volumes estimation for all available datasets compared with literature data. The asterisk indicates that 2017 estimation lacks of data from one station with respect to 2018. RG, gauging station; PR, point RaDAR; ZR, zonal RaDAR.

Tab. 2 - Volumi di infiltrazione calcolati per tutti i dataset disponibili confrontati con i dati da letteratura. L'asterisco indica che le valutazioni 2017 sono state effettuate con una stazione in meno rispetto al 2018. RG, pluviometro; PR, RaDAR puntuale; ZR, RaDAR zonale .

2017*	Mm^3/yr			2018	Mm^3/yr			Experimental literature data	Mm^3/yr
	Turc	Turc mod	Thornthwaite		Turc	Turc mod	Thornthwaite		
RG	432	458	419	RG	367	369	350	Nanni & Rusi 2003	252
PR	100	118	76	PR	179	185	160		
ZR (min)	133	134	99	ZR (min)	124	121	101		
ZR (max)	231	232	203	ZR (max)	223	228	207		
ZR (mean)	182	181	149	ZR (mean)	170	170	151		

Discussion

Comparison between rainfall data

A comparison between gauging rainfall data and weather RaDAR data has been put together using charts. Figure 5a and 5b show the comparison between real gauging stations data and weather RaDAR data and between virtual gauging stations data and RaDAR ones, respectively. As can be seen in Figure 5a, a good correspondence can be found in PAL, PTR and CSD's rainfall data: weather RaDAR data have slight differences with meteorological stations ones. In CRM, GUR, and PLN, the two trends are very similar but weather RaDAR data underestimate rain gauges values. Observing zonal-sampled data, mean and maximum weather RaDAR rainfall values are close to gauging stations ones.

This underestimation can be explained with the different recording methods of gauging station and weather RaDAR: the first collects rain data in a single point and not considering the surrounding area, while the last records data in a big volume and it cannot detect intense rain contrary to automatic gauge stations. Furthermore, points far from the RaDAR sensors will have a lower resolution and accuracy than a near ones.

Considering the charts in Figure 5b, the TRO*, MFO*, and MAR* stations, located at high elevations, reveal the biggest discrepancy between the two datasets: rain gauges data are significantly greater than weather RaDAR ones, likely related to the acquisition method and all the post-processing phases or to an effective minor value of precipitation considering that TRO*, MFO*, and MAR* are virtual stations. This can be explained considering that the virtual stations data can be overestimated, and RaDAR ones can be underestimated; virtual stations datasets have been reconstruct using a linear regression line build on rain data collected from the closest stations and assuming that higher altitudes mean higher rain values; it cannot be excluded that a better correlation can be applied, like a logarithmic one; this last correlation would involve an improvement in rainfall values less sharp than the linear one. On the other side, RaDAR data are direct measures, even if all its limitations need to be taken to account. In general, both RaDAR data and rain gauge stations follow the same temporal rainfall pattern. Meteorological station datasets are not always complete: an example is the GUR station (see Fig.5a). In 2017 this gauging station did not work, while for 2018 it has only collected data from May to December; another example is PTR where October 2018 is missed.

The major differences between the two types of rainfall data have been explained in Figure 4: weather data have a range of rainfall value inside every Thiessen polygon, while rainfall data describe an unchanging value all over the single polygon. This feature makes weather RaDAR data more solid than those from the inhomogeneous distribution of the rain gauges. Weather RaDAR rain products are more effective than rain gauge network in catching the spatial variability of the meteoric events, which is certainly useful for the water budget calculation at local scale.

Comparison between aquifer potential recharge estimations

Figure 6 shows the difference between potential recharge estimation calculated with data from rain gauge network and weather RaDAR. Both have been compared with literature data (Nanni and Rusi 2003); the authors have estimated infiltration volumes using Turc and Thornthwaite methods over a 40-years period (1952-1992), 18 gauging stations and direct discharge measurements. Obtained discharge volumes are 263 Mm^3/yr (Turc methods), 244 Mm^3/yr (Thorthwaite), 252 Mm^3/yr (discharge measurements). Rain gauge

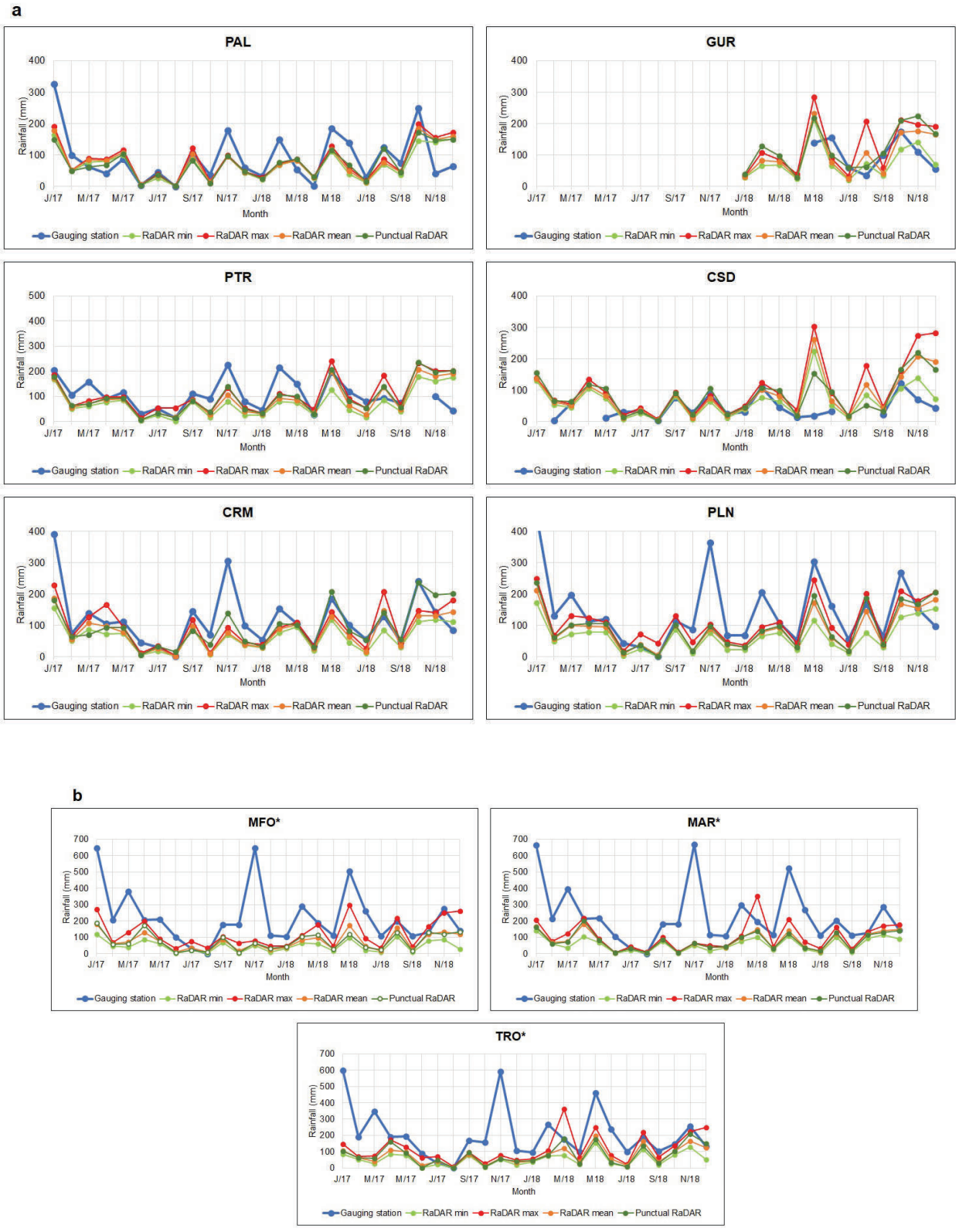

Fig. 5 - a) Comparison between real gauging stations rainfall data (blue) and RaDAR rain data (other colors). b) Comparison between virtual gauging stations rainfall data (blue) and RaDAR data (other colors).

Fig. 5 - a) Confronto tra piogge misurate dai pluviometri (blu) e piogge rilevate dal RaDAR meteorologico (altri colori). b) Confronto tra piogge misurate dai pluviometri fittizi (blu) e piogge rilevate dal RaDAR meteorologico (altri colori).

estimations are higher than the other one for both years as it could have been expected from previous observations. On the other hand, the comparative analysis with the experimental data from literature, although referring to different study periods, shows a good correspondence with the data obtained from the maximum values of weather RaDAR datasets.

Conclusion

The article focuses on the well-known Majella massif in Central Italy to test the feasibility of estimating the groundwater budget in regional aquifers through weather RaDAR data and comparing RaDAR estimates with rain gauge ones. The first results of the study, carried out for the period between 2017 and 2018, have shown in general that the calculations are, at the present time, expensive in terms of time and hardware, the weather RaDAR data shows lower values than those obtained by rain gauges, and a major homogeneity in the distribution of the precipitation respect to the altitude.

From a quantitative point of view, the evaluation of precipitation showed a good correlation between data from real rain gauges and data from weather RaDAR, while, for virtual stations, the data from rain gauges are more than twice. This situation considerably influences the estimate of the aquifer potential recharge, considering that the areas with virtual rain gauges are the largest and where most of the infiltration occurs. On the other hand, the comparative analysis between the potential recharge estimation from weather RaDAR data and the recharge experimental data from literature, although referring to different study periods, shows a good correspondence.

Even though simplified, the comparison methods (i.e., points and Thiessen polygons) provided meaningful results, as they represent common data supports for two different types of rainfall dataset (i.e., point and raster data) that would have not been possible to compare otherwise.

In the end, to further evaluate whether he data from weather RaDAR are underestimated, or the data from the rain gauges are overestimated, it will be useful to carry out further elaborations and comparisons with hydrogeological balance in other well-known aquifer and hydrological balance in well-known catchment area.

Acknowledgement

Durante la fase di revisione di questo lavoro è venuto improvvisamente a mancare il collega coautore ed amico Frank Silvio Marzano. Con il suo competente contributo il lavoro è stato pensato e progettato, senza il suo infaticabile supporto non avrebbe visto la luce. Grazie Frank, per questo e per tutto il resto.

Funding

This research received no external funding.

Competing interest

The authors declare no competing interest.

Author contributions

Conceptualization, SR and DDC; collection of data, DDC, ADG, FM, RL; data processing, ADG, DDC, RL; interpretation of results, SR, DDC, ADG, FM, RL; writing-original draft preparation, ADG; writing-review and editing, SR, ADG, DDC, FM, RL; supervision, SR.

Additional information

Supplementary information is available for this paper at https://doi.org/10.7343/as-2022-568

Reprint and permission information are available writing to acquesotterranee@anipapozzi.it

Publisher's note Associazione Acque Sotterranee remains neutral with regard to jurisdictional claims in published maps and institutional affiliations.

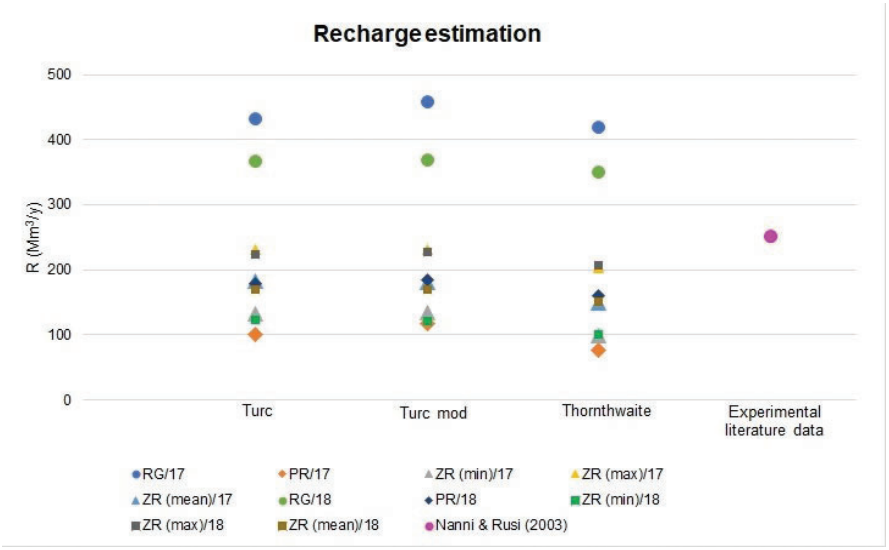

Fig. 6 - Recharge estimation comparison between gauging stations data (RG), point RaDAR (RP), the three values from zonal RaDAR (ZR) for both 2017 and 2018 and the experimental literature data from Nanni and Rusi (2003).

Fig. 6 - Confronto dei valori di ricarica tra dati da pluviometro (RG), da RaDAR puntuale (PR), i tre valori del RaDAR areale (ZR) per 2017 e 2018 e i dati sperimentali da Nanni e Rusi (2003).

REFERENCES

Andreo B, Vías J, Durán JJ, Jiménez P, López-Geta JA, Carrasco F (2008) Methodology for groundwater recharge assessment in carbonate aquifers: application to pilot sites in southern Spain. Hydrogeology Journal. doi:10.1007/s10040-008-0274-5

Barbieri S, Di Fabio S, Lidori R, Rossi FL, Marzano FS, Picciotti E (2022) Mosaicking Weather Radar retrievals from an Operational Heterogeneous Network at C and X Band for Precipitation Monitoring in Italian Central Apennines. Remote Sens. doi:10.3390/rs14020248

Boni C, Bono P, Capelli G (1986) Schema idrogeologico dell'Italia Centrale *"Hydrogeological scheme of Central Italy"*. Mem. Soc. Geol. It., 35 (2): 991-1012.

Celico P (1983) Idrogeologia dell'Italia centro meridionale *"Hydrogeology of south-central Italy"* Quad. Cassa Mezzog. 4: 1-225.

Chiaudani A, Di Curzio D, Palmucci W, Pasculli A, Polemio M, Rusi S (2017) Statistical and Fractal Approaches on Long Time-Series to Surface-Water/Groundwater Relationship Assessment: A Central Italy Alluvial Plain Case Study, Water. doi:10.3390/w9110850

Chiaudani A, Di Curzio D, Rusi S (2019) The snow and rainfall impact on the Verde spring behavior: A statistical approach on hydrodynamic and hydrochemical daily time-series. Science of The Total Environment. doi:10.1016/j.scitotenv.2019.06.433

Chilès JP, Delfiner P (2012) Geostatistics: Modeling Spatial Uncertainty. 2nd ed. Wiley, Hoboken, NJ, USA.

Di Curzio D, Rusi S, Di Giovanni A, Ferretti E (2021) Evaluation of Groundwater Resources in Minor Plio-Pleistocene Arenaceous Aquifers in Central Italy. Hydrology. doi:10.3390/hydrology8030121

Di Curzio D, Rusi S, Signanini P (2019) Advanced redox zonation of the San Pedro Sula alluvial aquifer (Honduras) using data fusion and multivariate geostatistics. Science of The Total Environment. doi:10.1016/j.scitotenv.2019.133796

Falconi MT and FS Marzano (2019) Weather RaDAR Data Processing and Atmospheric Applications: An overview of tools for monitoring clouds and detecting wind shear. IEEE Signal Processing Magazine. doi:10.1109/MSP.2019.2890934

Fiorillo F, Petitta M, Preziosi E, Rusi S, Esposito L, Tallini M (2015) Long-term trend and fluctuations of karst spring discharge in a Mediterranean area (central-southern Italy). Environmental Earth Sciences. doi:10.1007/s12665-014-3946-6

Fronzi D, Di Curzio D, Rusi S, Valigi D, Tazioli A (2020) Comparison between Periodic Tracer Tests and Time-Series Analysis to Assess Mid-and Long-Term Recharge Model Changes Due to Multiple Strong Seismic Events in Carbonate Aquifers. Water. doi:10.3390/w12113073

Harrison DL, Driscoll SJ, Kitchen M (2000) Improving precipitation estimates from weather radar using quality control and correction techniques. Meteorol. Appl. doi:10.1017/s1350482700001468

Lorenzi V, Sbarbati C, Banzato F, Lacchini A, Petitta M (2022) Recharge assessment of the Gran Sasso aquifer (Central Italy): Time-variable infiltration and influence of snow cover extension. Journal of Hydrology: Regional Studies. doi:10.1016/j.ejrh.2022.101090

McKee JL, Binns AD (2016) A review of gauge–radar merging methods for quantitative precipitation estimation in hydrology, Canadian Water Resources Journal / Revue canadienne des ressources hydriques. doi:10.1080/07011784.2015.1064786

Montopoli M,Picciotti E, Baldini L, Di Fabio S, Marzano F S, Vulpiani G (2021) Gazing inside a giant-hail-bearing Mediterranean supercell by dual-polarization Doppler weather RaDAR. Atmospheric Research. doi:10.1016/j.atmosres.2021.105852.

Nanni T, Rusi S (2003) Idrogeologia del massiccio carbonatico della montagna della Majella (Appennino centrale) *"Hydrogeology of Majella Mountain carbonatic massif (Central Appennines)"* Boll. Soc. Geol. It., 122: 173-202, 27 ff., 9 tabb., 2 tavv. f.t.

Navarro A, García-Ortega E, Merino A, Sánchez JL, Tapiador FJ (2020) Orographic biases in IMERG precipitation estimates in the Ebro River basin (Spain): The effects of rain gauge density and altitude. Atmospheric Research. doi:10.1016/j.atmosres.2020.105068

Petitta M, Scarascia Mugnozza G, Barbieri M, Bianchi Fasani G, Esposito C (2010) Hydrodynamic and isotopic investigations for evaluating the mechanisms and amount of groundwater seepage through a rockslide dam. Hydrological Processes. doi:10.1002/hyp.7773

Thiessen AH (1911) Precipitation average for large areas. Monthly weather rev.

Thornthwaite CW, Mather JR (1957) Instruction and Tables for computing potential evapotraspiration and water balance. Public. Climatology, 10: 185-311.

Tondi E, Antonellini M, Aydin A, Marchegiani L, Cello G (2006) The role of deformation bands, stylolites and sheared stylolites in fault development in carbonate grainstones of Majella Mountain, Italy. Journal of Structural Geology. doi:10.1016/j.jsg.2005.12.001.

Turc L (1954) Le bilan d'eau des sols: relation entre les précipitations, l'évaporation et l'écoulement *"Soil water budget: relationship between rainfall, evaporation and outflow"*. La Houille blanche, 3 journèes de l'hydraulique de la Societè Hydrotecnique de France, Paris, 36-44.

Vessia G, Di Curzio D, Castrignanò A (2020) Modeling 3D soil lithotypes variability through geostatistical data fusion of CPT parameters. Science of the Total Environment. doi:10.1016/j.scitotenv.2019.134340

Viaroli S, Di Curzio D, Lepore D, Mazza R (2019) Multiparameter daily time-series analysis to groundwater recharge assessment in a caldera aquifer: Roccamonfina Volcano, Italy. Science of the Total Environment. doi:10.1016/j.scitotenv.2019.04.327

Viaroli S, Mastrorillo L, Lotti F, Paolucci V, Mazza R (2018) The groundwater budget: a tool for preliminary estimation of the hydraulic connection between neighboring aquifers. Journal of hydrology. doi:10.1016/j.jhydrol.2017.10.066

Vulpiani G, Montopoli M, Delli Passeri L, Gioia AG, Giordano P, Marzano FS (2012) On the use of dual-polarized C-band RaDAR for operational rainfall retrieval in mountainous areas, J. Appl. Meteor. Climat. doi:10.1175/JAMC-D-10-05024.1.

Wackernagel H (2003) Multivariate Geostatistics: An Introduction with Applications. Springer-Verlag, Berlin.